In Vivo NIR Fluorescence Imaging, Biodistribution, and Toxicology of Photoluminescent Carbon Dots Produced from Carbon Nanotubes and Graphite

Huiquan Tao, Kai Yang, Zhen Ma, Jianmei Wan, Youjiu Zhang, Zhenhui Kang,* and Zhuang Liu**

Oxidization of carbon nanotubes by a mixed acid has been utilized as a standard method to functionalize carbon nanomaterials for years. Here, the products obtained from carbon nanotubes and graphite after a mixed-acid treatment are carefully studied. Nearly identical carbon dot (Cdot) products with diameters of 3–4 nm are produced using this approach from a variety of carbon starting materials, including single-walled carbon nanotubes, multiwalled carbon nanotubes, and graphite. These Cdots exhibit strong yellow fluorescence under UV irradiation and shifted emission peaks as the excitation wavelength is changed. In vivo fluorescence imaging with Cdots is then demonstrated in mouse experiments, by using varied excitation wavelengths including some in the near-infrared (NIR) region. Furthermore, in vivo biodistribution and toxicology of those Cdots in mice over different periods of time are studied; no noticeable signs of toxicity for Cdots to the treated animals are discovered. This work provides a facile method to synthesize Cdots as safe non-heavy-metal-containing fluorescent nanoprobes, promising for applications in biomedical imaging.

1. Introduction

Semiconductor quantum dots (QDs) have generated much excitement for their various potential applications in optical bioimaging and beyond.[1] Because of the excellent photostability, shape emission bands, and tunable emission wavelengths, QDs are generally considered as an alternative of conventional organic dyes and genetically engineered fluorescent proteins in fluorescence imaging of certain biological samples.[2–7] However, most traditional QDs contain group VI heavy metal elements, which raise significant concerns regarding the potential toxicity of using those nanomaterials in biological systems.[8–11] Considerable efforts have been devoted to the development of heavy-metal-free novel photoluminescence nanoprobes in the past several years.[12,13] Carbon nanoparticles or carbon dots (Cdots) as a class of 'zero-dimensional' carbon nanomaterials possess some of the same major advantageous characteristics of semiconductor QDs, such as high photostability, tunable emission, and large two-photon excitation cross-sections.[2,12–15] Moreover, compared with semiconductor QDs, Cdots exhibit nonblinking fluorescence, excellent water solubility, and are cheaply produced.[12–14,16–19] Most importantly, Cdots without heavy metal content are more environmental friendly and could be much safer for biological use.[15,19,20]

As the result, a number of groups have studied the synthesis of Cdots as well as the applications of Cdots in bio-imaging. In view of the significant potential of luminescent Cdots in various fields, a facile and scalable synthetic approach is highly desired. Following the laser ablation method,[12] various strategies have been established to

H. Q. Tao,[+] K. Yang,[+] Z. Ma, Prof. Z. H. Kang, Prof. Z. Liu
Functional Nano & Soft Materials Laboratory (FUNSOM)
Jiangsu Key Laboratory for Carbon-Based
Functional Materials & Devices Soochow University
Suzhou, Jiangsu, 215123 China
E-mail: zliu@suda.edu.cn; zhkang@suda.edu.cn
Dr. J. M. Wan, Prof. Y. J. Zhang
School of Radiation Medicine and Public Health Soochow University
Suzhou, Jiangsu 215123, China
E-mail: yjzhang@suda.edu.cn
[+] These authors contributed equally to this work

DOI: 10.1002/smll.201101706

produce carbon nanoparticles, including electrochemical release or exfoliation from a graphitic source, separation of combusted carbon soot by centrifugation and denaturing polyacrylamide gel electrophoresis (PAGE), carbonizing polymerized resols on silica spheres, thermal oxidation of suitable molecular precursors, and dehydration of carbohydrates using concentrated sulfuric acid.[14,16,17,21–26] However, many of these synthetic methods are relatively tedious. A concise approach to generate Cdots would be attractive.

On the other hand, owing to their photoluminescent feature, Cdots have been widely studied for optical bioimaging in vitro and in vivo.[12,13,20,27] However, most of those fluorescent imaging studies were carried out under UV or visible excitation. To the best of our knowledge, in vivo imaging in the near-infrared (NIR) region (700–900 nm), in which the tissue transparency window is ideal for in vivo optical imaging, has not yet been reported using Cdots. Moreover, although a previous pilot study showed that Cdots were not obviously toxic to treated mice,[19] a systematic investigation on the pharmacokinetics, biodistribution, and toxicology of this type of nanomaterials is still required.

Oxidizing carbon nanotubles (CNTs) using a mixed acid is a standard method to cut and functionalize nanotubes.[28,29] The by-product of this process, which is a tan transparent liquid with yellow fluorescence under UV light, was previously considered to comprise ultrashort CNTs.[28,30] Recently, Tour and co-workers reported a new way to obtain carbon nanoparticles from single-walled carbon nanotubes (SWNTs). In their work, SWNTs was treated by oleum and then nitric acid, yielding a solution of carbon nanoparticles, referred to as hydrophilic carbon clusters (HCCs), which were used as nanovectors for drug delivery.[31,32]

Inspired by their findings, we studied the oxidization by-products of CNTs and graphite, and we find the previously named 'ultrashort' CNTs are in fact 3–5 nm HCCs or Cdots with tunable fluorescence emissions under different excitation wavelengths. Surprisingly, the optical absorbance and fluorescence emission spectra of Cdots prepared by different carbon sources including SWNTs, multiwalled carbon nanotubes (MWNTs), and graphite are nearly identical. We then chose Cdots prepared from MWNTs for in vivo biological studies. It is shown that our Cdots could serve as novel fluorescent probes for in vivo imaging in live mice by using a wide range of excitation wavelengths, with excellent signal-to-background separation under NIR excitation. In an unprecedented work, we further study the in vivo biodistribution of Cdots by a radiolabeling method. After intravenous injection, the Cdots exhibit high accumulation in the reticuloendothelial system (RES) as well as in the kidney, and they are gradually excreted via both renal and fecal pathways. Importantly, we observe that Cdots at a dose of 20 mg/kg appear to be safe to the treated animals over a period of 3 months as evidenced by the systematic time-course blood chemical analysis and complete blood panel and histological analyses. Our work demonstrates a rather simple approach to produce nontoxic fluorescent Cdots with great potential in biological imaging applications.

2. Results and Discussion

2.1. Preparation of Cdots

Two types of carbon nanotubes (SWNTs, MWNTs) and graphite were oxidized by a mixed acid (sulfuric acid:nitric acid = 3:1, **Figure 1**A); this has been a standard method to functionalize carbon nanotubes for many years. After 24 h of refluxing, the mixture was slowly dispersed in 100 mL deionized water and filtered with a 0.1 μm filter to remove CNTs and graphite residues. The filtrate was then dialyzed in a 14 000 Da dialysis bag against deionized water to remove excess acids. We obtained a tan transparent liquid that emitted bright yellow fluorescence under UV light (365 nm) (Figure 1B). The obtained solutions were rather stable in physiological solutions; they did not contain any sediments after being incubated in saline, fetal bovine serum (FBS), or FBS containing cell medium for 48 h (Figure 1C). Notably, the Cdots solution could be stored at room temperature for as long as one year, without the formation of any precipitates or the loss of fluorescence (Figure 1C, Inset).

2.2. Characterization

We next characterized the morphology of the filtrate products prepared from CNTs and graphite using atomic force microscopy (AFM) (Figure 1D). AFM images of all three samples revealed that the products were small nanoparticles with diameters in the range of ~2–3 nm (determined by the AFM measured height). Transmission electronic microscopy (TEM) images of all three samples displayed spherical nanoparticles with diameters of ~3–5 nm without any tubular structures (Supporting Information Figure S1). At a pH of 6.0, zeta potentials were measured to be –28.0, –32.85, and –34.7 mV for Cdots made from MWNTs (Cdots-M), SWNTs (Cdots-S), and graphite (Cdots-G), respectively. The elemental analysis data revealed that those Cdots had a high oxygen content (55%, calculated, Supporting Information Table S1), which was similar to Cdots synthesized from a nitric-acid treatment of candle soot.[23] The Fourier-transformed infrared (FTIR) spectroscopy evidenced the presence of carbonyl and hydroxyl groups (C=O: ~1730 cm^{-1}; O–H: ~3500 cm^{-1}, Supporting Information Figure S2), which make these Cdots highly water-soluble and could potentially allow for further bioconjugation.[31,32] It is worth noting that the procedure used in this case is very close to that used by Tour and co-workers in their previous studies,[31,32] and our products have similar properties to that of the HCCs reported in their work. Therefore, we suggest that the Cdots prepared by oxidization of various carbon materials are likely identical to HCCs.

The optical properties of Cdots-S, Cdots-M, and Cdots-G were characterized. All three types of Cdots showed similarly broad absorption in the UV–vis range (**Figure 2**A). The fluorescence emission spectra of Cdots showed shifted emission peaks as the excitation wavelength was changed. The fluorescence emission of the Cdots is attributed to the poly-aromatic sp^2 carbon nanostructures in the Cdot, as well as the various surface functional groups on the nanoparticles.[12,13] The excitation-dependent fluorescence emission behavior of our

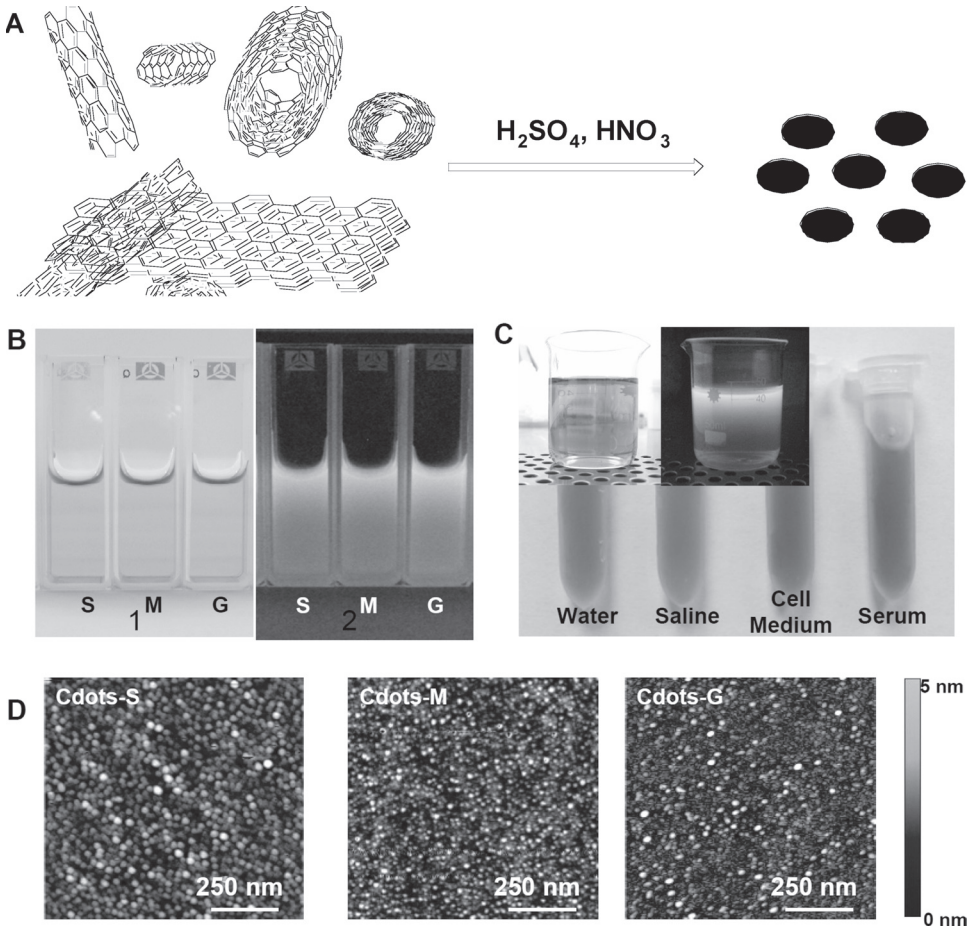

Figure 1. Synthesis of Cdots from various carbon sources. A) Schematic diagram of reactions. B) Solutions of Cdots-S, Cdots-M, and Cdots-G under ambient (left) and UV light (right). C) The stability of Cdots-M in different physiological solutions including water, saline (0.9% NaCl), RPMI-1640 cell medium, and fetal bovine serum. Inset: Photos of Cdots-M after being stored at room temperature for 1 year taken under ambient (left) and UV light (right). D) Atomic force microscopy (AFM) images of Cdots produced from three different carbon sources.

Cdots is similar to many previous reports,[12,23,25] and are likely due to the varied sizes of aromatic domains in Cdots. Under excitation at 460 nm, Cdots exhibited a maximum emission at 535 nm. Interestingly, all three types of Cdots prepared from different carbon sources showed very similar fluorescence properties (Figure 2B–D). The fluorescence quantum yield (QY) of Cdots was measured to be ~3–6%. We compared the photostability of Cdots with that of a commonly used fluorescent dye, fluorescein, by exposing these two solutions under a high-brightness cold light (350 W) for 6 h. The fluorescence of fluorescein decreased by 60% in 2 h, and almost disappeared after 6 h of light exposure. In marked contrast, no photobleaching of Cdots-M fluorescence was observed even after it was exposed to the same light for 24 h (Figure 2E,F).

2.3. Cytotoxicity

Before further use of Cdots for biological studies, we tested the in vitro cytotoxicity of three different Cdots using the human kidney embryonic 293T cell line. Varied concentrations of Cdots made from different original materials were added to the cells cultured in 96 well-plates and incubated for 24 h. Subsequently, a standard assay was performed to assess the cell viabilities after various Cdots treatments. No significant reduction in cell viability was observed for cells treated with Cdots even at ultrahigh concentrations (up to 0.5 mg/mL), demonstrating that the Cdots produced by our method were not obviously toxic in vitro (**Figure 3**).

2.4. In Vivo Optical Imaging

Cdots-M that were made from MWNTs were chosen for in vivo fluorescence imaging studies. A nude mouse was subcutaneously administered with Cdots-M at three different locations. The mouse was then anesthetized by intraperitoneal injection of 1% pentobarbital and imaged by a Maestro in vivo optical imaging system. Various excitations including blue, green, yellow, orange, red, deep red, and NIR light with center wavelengths at 455, 523, 595, 605, 635, 661, and 704 nm, respectively, were applied during in vivo imaging of the mouse. After spectral unmixing to differentiate the background autofluorescence (green), the subcutaneously injected spots (red) on the mouse were seen in those fluorescence images under all different excitation light (**Figure 4**).

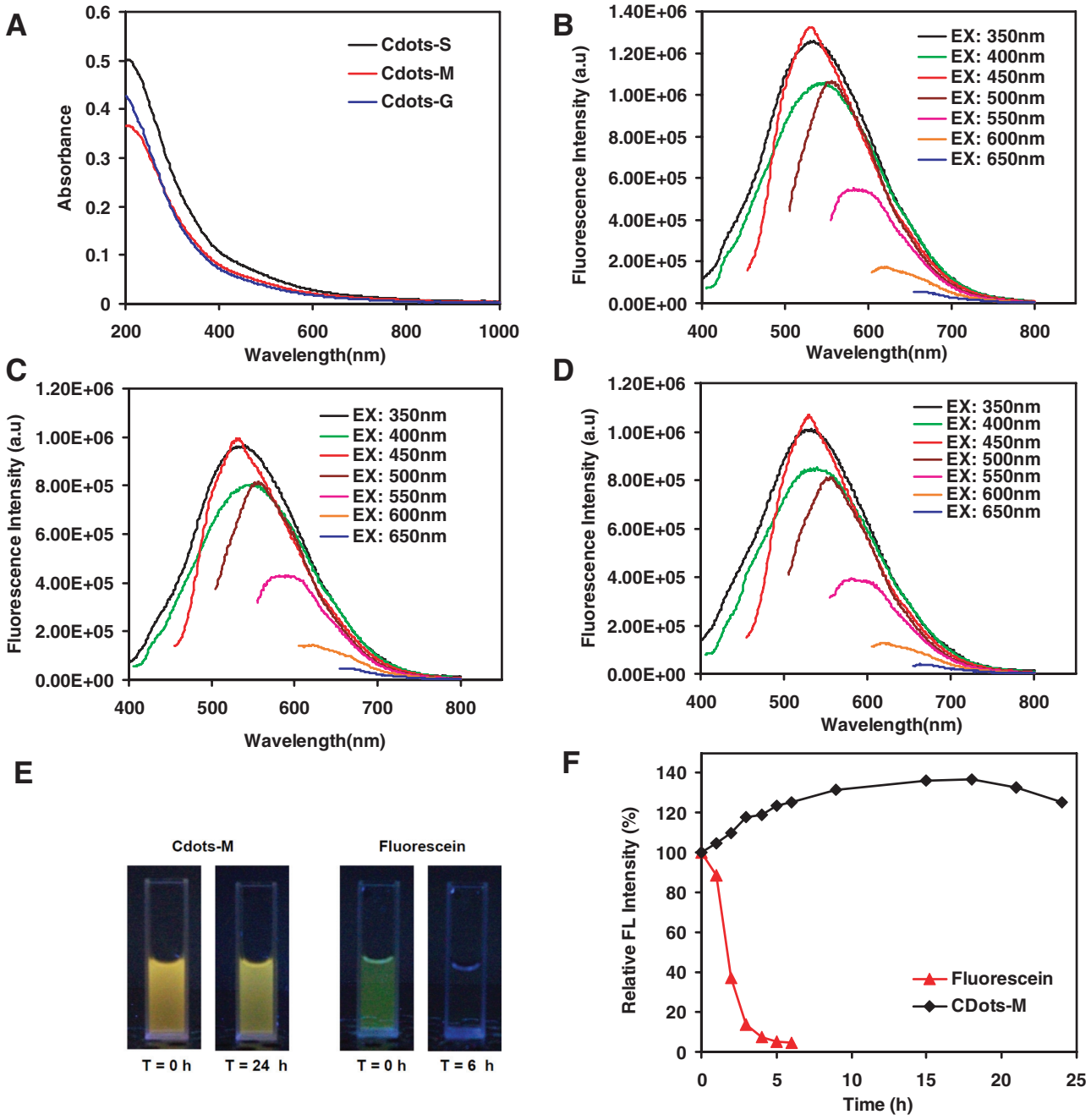

Figure 2. Optical properties of Cdots. A) UV–vis spectra of Cdots-S, Cdots-M, and Cdots-G. B–D) Fluorescence spectra of Cdots-S (B), Cdots-M (C), and Cdots-G(D) under varied excitation wavelengths. EX refers to the excitation wavelength. E) Photos of Cdots-M and fluorescein under UV light before and after being exposed to the high-brightness cold light source. T refers to the time of exposure. F) Photostability comparison of Cdots-M and fluorescein under the high-brightness cold light source over time.

Compared to images acquired using blue (455 nm) and green (523 nm) light excitation, those taken under longer-wavelength excitation (595 nm and beyond) showed much better signal-to-background separation. Although the fluorescence emission of Cdots is weaker at longer wavelengths, the tissue autofluorescence background decreases even more, resulting in an improved signal-to-noise ratio under red and NIR excitations. In vivo optical imaging at longer wavelengths is usually preferred owing to the improved photon tissue penetration and reduced background autofluorescence, especially if in the NIR region. The capability of using our Cdots for NIR in vivo fluorescence imaging (excitation = 704 nm, emission = 770 nm) indicates their great promise for future use as optical nanoprobes in biomedical imaging.

2.5. Blood Circulation and Biodistribution of Radiolabeled Cdots

In order to track Cdots in vivo, we labeled Cdots-M with ^{125}I using a strategy similar to the ^{125}I-labeling of carbon

small NANO MICRO

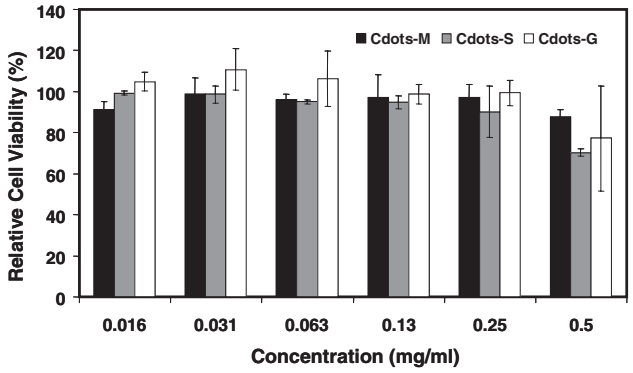

Figure 3. Relative viabilities of 293T cells (normalized to the untreated control) after being incubated with Cdots at varied concentrations for 24 h. Error bars were based on standard deviations of triplicated samples.

nanotubes and graphene.[33–35] In such a reaction, iodine atoms (after being oxidized from I^- by chloramine T) are likely attached to the aromatic rings of sp^2 nanocarbons via electrophilic addition.[33–35] The radiolabeling stability of ^{125}I-Cdots-M was tested in mouse plasma at 37 °C for 7 days (**Figure 5**A), revealing an acceptable amount of ^{125}I detachment from Cdots (less than 20% of ^{125}I fell off from carbon dots in the mouse plasma at 37 °C over 7 days). The decent radiolabeling stability of ^{125}I-Cdots-M allows tracking and detection of Cdots in animals over a certain period of time (e.g., within a week).

To understand the pharmacokinetics of Cdots, we first measured radioactivity levels in the blood over time (Figure 5B) after intravenous injection of ^{125}I-Cdots-M into Balb/c mice (4 mg/kg, 20 μCi). Blood was drawn from the tail veins of mice at different time points post-injection (p.i.), and measured by a gamma counter. The ^{125}I-Cdots-M level in the blood was determined by the standard unit, the percentage of injected dose per gram tissue (%ID/g). The blood circulation of ^{125}I-Cdots-M followed a two-compartment model, with the first- and second-phase circulation half-lives at 0.10 ± 0.09 and 2.1 ± 0.3 h, respectively.

Next, we studied the biodistribution of ^{125}I-Cdots-M. Female Balb/c mice were sacrificed at 5 h, 1 day, 3 days, or 7 days after the injection of ^{125}I-Cdots-M (4 mg/kg, 20 μCi). Various organs and tissues were collected and measured by the gamma counter. It was found that Cdots mainly accumulated in the RES organs, such as liver and spleen (Figure 5C) after intravenous injection, similar to the in vivo behaviors of many other nanomaterials used in biomedicine.[33,34,36,37] Distinctively, owing to the ultrasmall size (2–5 nm) of our Cdots,[38] the kidney uptake of Cdots is rather high at early time points, indicating that Cdots likely could pass the glomerulus and be excreted by urine. An obvious trend of decreasing radioactivities in all organs was observed from the biodistribution data, possibly due to the clearance of Cdots from the mouse body. We then used metabolism cages to collect urine and feces of mice after injection of ^{125}I-Cdots-M (Figure 5D). High radioactivities were measured in urine and feces samples, suggesting that the clearance of Cdots was possibly through both renal and fecal excretions.

One concern for in vivo biodistribution studies based on the radiolabeling method is the potential detachment of radioisotope from the labeled materials. In our system, the labeled ^{125}I-Cdots-M was rather stable in mouse plasma at 37 °C. We also carried out a control study by injecting free Na^{125}I into mice, and discovered that the majority of

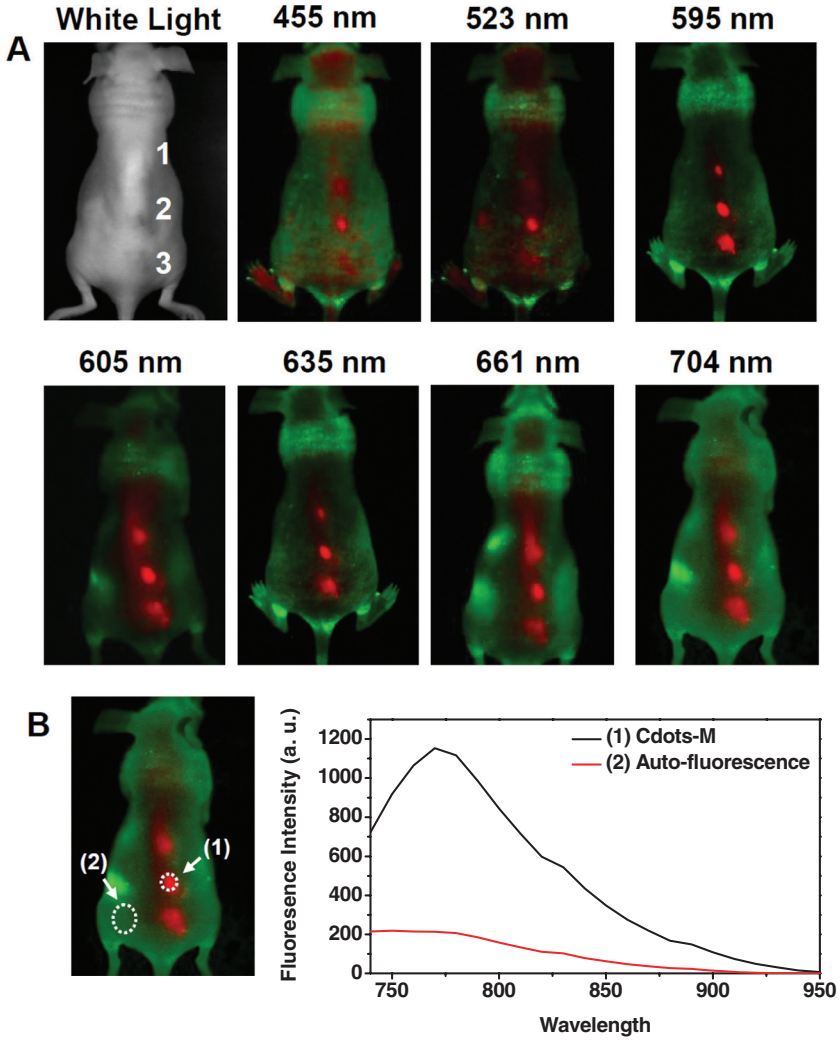

Figure 4. In vivo fluorescence imaging. A) In vivo fluorescence images of a Cdots-M-injected mouse. The images were taken under various excitation wavelengths at 455, 523, 595, 605, 635, 661, and 704 nm. Red and green represent fluorescent signals of Cdots-M and the tissue autofluorescence, respectively. B) Signal-to-background separation of the spectral image taken under the NIR (704 nm) excitation. The Cdots fluorescence was well separated from the tissue autofluorescence background.

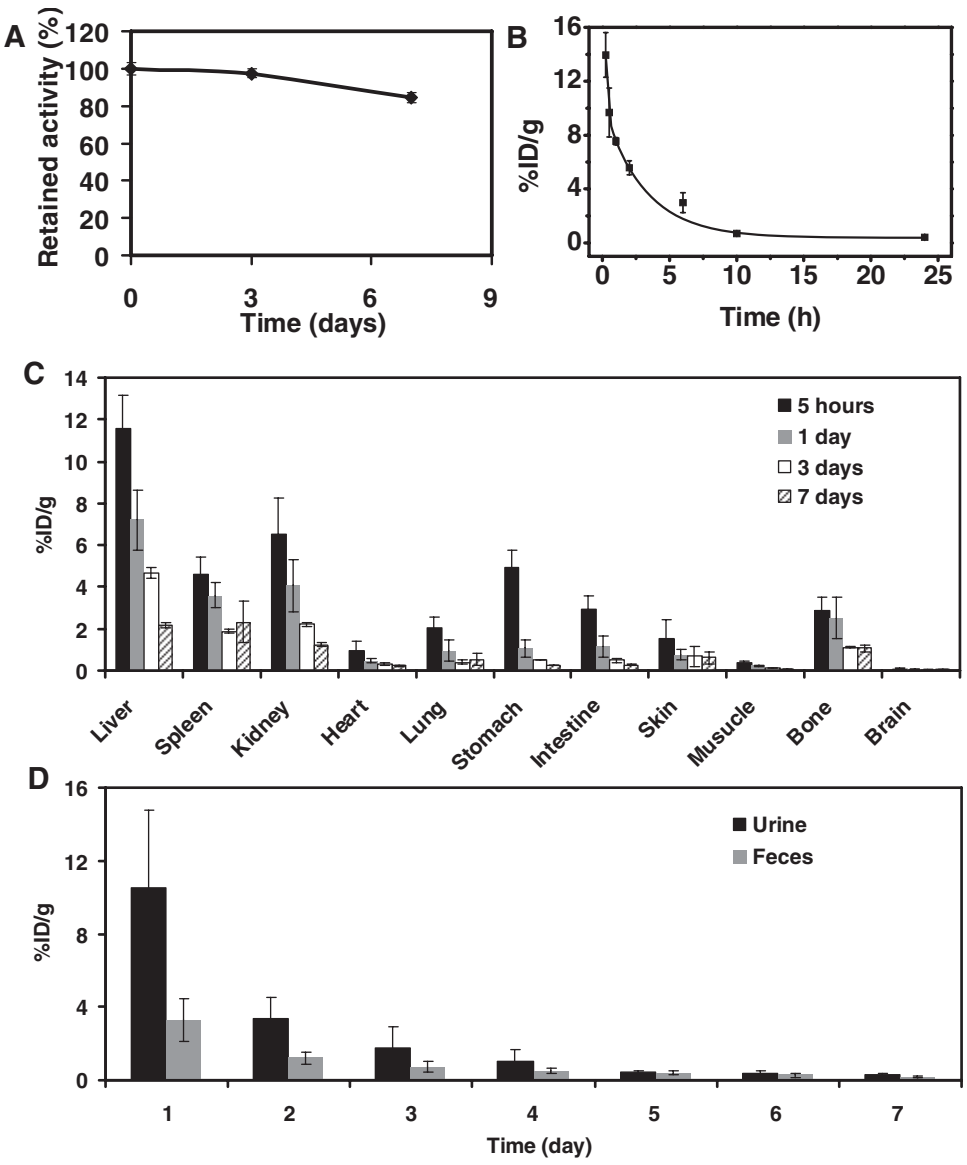

Figure 5. Pharmacokinetics and biodistribution of ^{125}I-Cdots-M in mice. A) The radiolabeling stability curve of ^{125}I-Cdots-M in mouse plasma at 37 °C. B) The blood circulation curve of ^{125}I-Cdots-M. C) Time-dependent biodistribution of ^{125}I-Cdots-M in female Balb/c mice. D) Distribution of ^{125}I-Cdots-M in urine and feces of Balb/c mice collected by metabolism cages. Error bars were based on standard deviations of four mice per group.

radioactivity was excreted within 5 h with minimal amount of retention in various organs, except for in the stomach and thyroid (Supporting Information Figure S3). The biodistribution between free ^{125}I and ^{125}I-Cdots-M differed drastically. Although it is possible that ^{125}I could still be gradually detached from ^{125}I-Cdots-M in vivo over time, this radiolabeling method is still a viable tool to understand the in vivo behaviors of Cdots at least in short term.

2.6. In Vivo Toxicology

The potential toxic effect is a major concern when using nanomaterials in biomedicine. We systematically investigated the in vivo toxicology of Cdots-M to female Balb/c mice over 3 months. During our experiments, we did not notice any obvious sign of toxic side effect for Cdot-injected mice at the dose of 20 mg/kg within 90 days. Neither death nor significant body weight drop was noted in the treatment group (**Figure 6**).

To reveal any potential toxic effects of Cdots to the treated mice, we carried out blood biochemistry and hematology analysis. Mice injected with Cdots-M (20 mg/kg, unlabeled) were sacrificed at 1 day, 7 days, 20 days, 40 days, and 90 days p.i. for blood collection (5 mice per group). Blood from age-matching control untreated mice was collected at day 3, 40, and 90 (5 mice per group). The blood levels of liver function markers, including alanine aminotransferase (ALT), aspartate aminotransferase (AST), alkaline phosphatase (ALP), and the ratio of albumin and globulin (A/G) of

NANO MICRO small

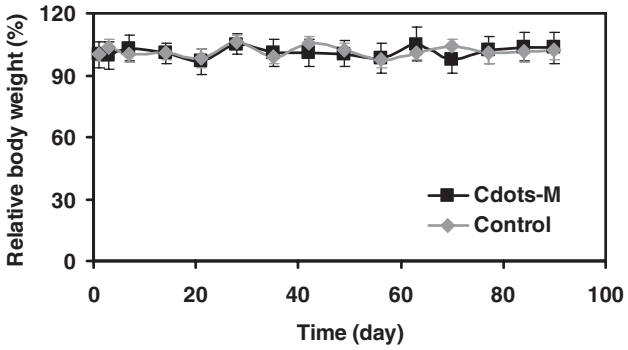

Figure 6. Mouse body weight data of the control group and the Cdots-M-injected group at the dose of 20 mg/kg. Mice in both groups during 90 days of observation showed no significant body weight drop.

Cdots-M treated mice, were all consistent to that of the control healthy mice, suggesting that no obvious hepatic toxicity was induced by Cdots treatment (**Figure 7**a,b). The blood urea level, which was an indicator of kidney functions, was also normal for treated mice (Figure 7c).[39] We selected the following important hematology markers for the hematological assessment: white blood cells, red blood cells, hemoglobin, mean corpuscular volume, mean corpuscular hemoglobin, mean corpuscular hemoglobin concentration, platelet count, and mean corpuscular hemoglobin (Figure 7d–k). All of the above parameters in the Cdots-M-treated mice at different p.i. times appeared to be normal compared with the control groups and in good agreement with the reference normal ranges.[39]

Careful necropsy was conducted 1, 7, 20, 40, and 90 days after injection of Cdots-M (no ^{125}I labeling) at the dose of 20 mg/kg; no obvious organ damage was noticed. We collected the main organs including liver, spleen, kidney, and heart of the mice from the control and treated groups, and sliced them for hematoxylin and eosin (H&E) staining (**Figure 8**). Overall no apparent histopathological abnormality or lesion in the treated groups at our injected Cdots dose was observed. Our results collectively suggest that Cdots at our injected dose are not noticeably toxic to the treated animals.

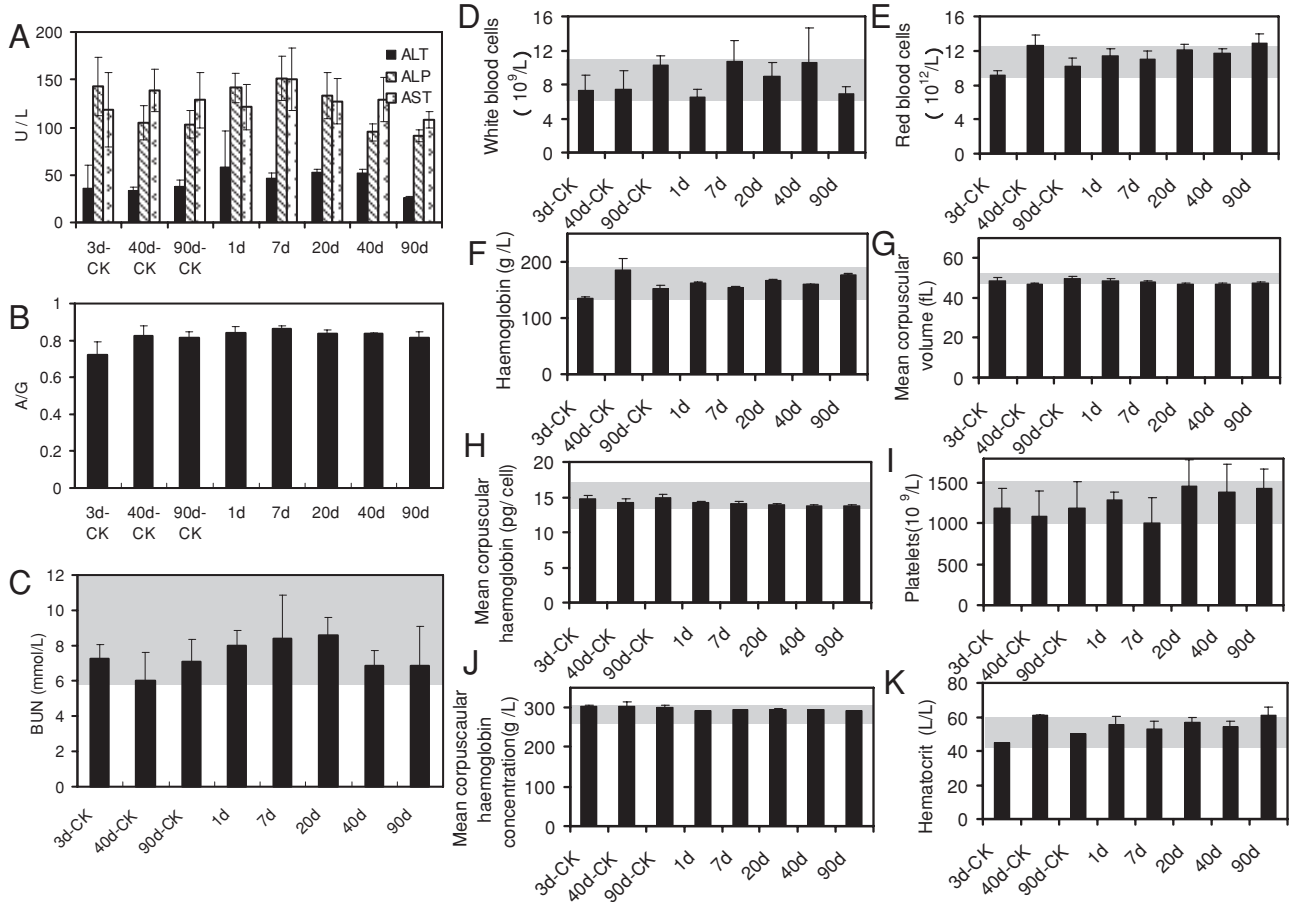

Figure 7. Blood biochemistry and hematology data of female Balb/c mice treated with Cdots-M at the dose of 20 mg/kg at 1, 7, 20, 40, and 90 days p.i. Age-matching untreated mice were sacrificed at 3, 40, and 90 day p.i. as controls (3d-CK, 40d-CK, and 90d-CK, respectively). A) ALT, ALP, and AST levels in the blood at various time points after Cdots-M treatment. B) Time-course albumin/globin ratios. Bloodchemistry data suggested no hepatic disorder induced by the Cdots-M treatment. C) Blood urea nitrogen (BUN) over time. D–K) Time-course changes of white blood cells (D), red blood cells (E), hemoglobin (F), mean corpuscular volume (G), meancorpuscular hemoglobin (H), platelets (I), mean corpuscular hemoglobin concentration (J), and hematocrit (K) from control mice and Cdots-M-treated mice. Statistics were based on 5 mice per data point. Gray areas in the figures show the normal reference ranges of hematology data of female Balb/c mice.

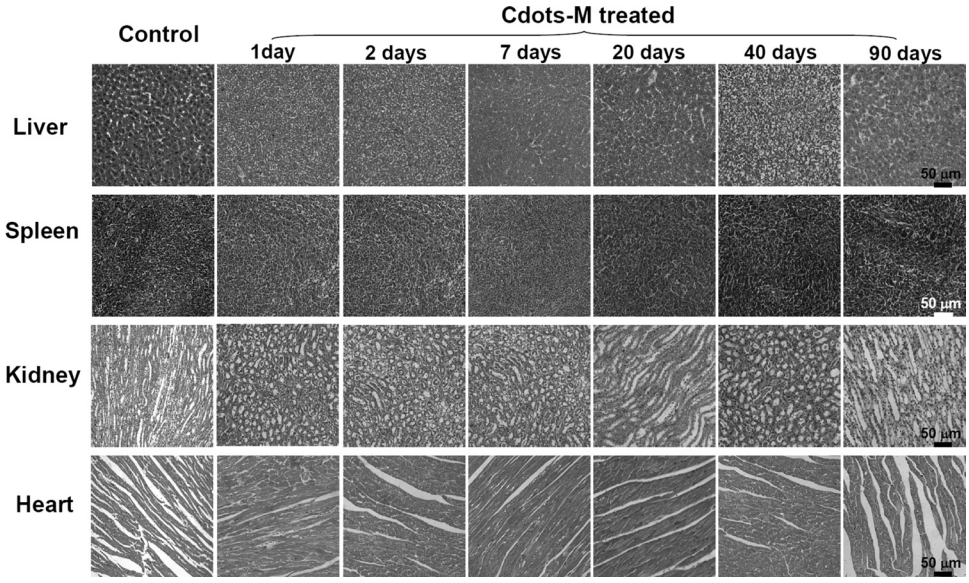

Figure 8. Representative H&E stained images of major organs, including liver, spleen, and kidney, collected from the control untreated mice and the Cdots-M-injected (20 mg/kg) mice at various time points post-injection. No noticeable abnormality or lesion was observed in organs of Cdot-treated mice.

3. Conclusion

In this work, we revisited the oxidization of CNTs by mixed acids, and we carefully studied the products in filtrate samples obtained from various carbon sources. Carbon dots (which could also be referred to as hydrophilic carbon clusters[31,32]) with similar sizes, morphologies, and optical properties were obtained from three different carbon materials: SWNTs, MWNTs, and graphite. For the first time, the photoluminescence of Cdots was demonstrated to be applicable for in vivo NIR fluorescence imaging in animals. The in vivo biodistribution of Cdots was also studied for the first time using a radiolabeling method. Although an alternative approach may be needed to understand the long-term in vivo fate of Cdots, our current data suggest the gradual clearance of Cdots from the mouse body, likely through both renal and fecal excretions. Furthermore, no obvious toxic effects of as-prepared Cdots to the treated mice were observed in our systematic time-course blood tests and histological analysis, encouraging further exploration of these nanomaterials in biomedicine. Further improvement of QY for our Cdots may be achieved by appropriate surface modification,[12,13,18,27] and is currently in progress in our laboratory. Nevertheless, our work demonstrates that Cdots prepared by such a simple method may have great potential as nontoxic fluorescent nanoprobes in biomedical imaging.

4. Experimental Section

Preparation of Cdot: Cdots were prepared from a range of carbon materials including SWNTs, MWNTs, and graphite. All CNT samples were purchased from Shenzhen Nanotech Port Co. Ltd (NTP) and used as received. The graphite (Hua Dong Graphite Manufactory) was grounded with NaCl solid and washed with water before further use. All three kinds of carbon materials were treated with a harsh oxidation procedure employing sulfuric and nitric acid. 100 mg of raw carbon materials were mixed with 15 mL sulfuric acid and 5 mL nitric acid in a 50 mL flask and sonicated for 30 min. The mixture was then refluxed for 24 h at 80 °C. After cooling down to room temperature, the reaction mixture was dispersed in 100 mL deionized water and filtered with a 0.1 μm microfilm filter. The solid residue was discarded while the filtrate was dialyzed in a dialysis bag with the molecular-weight cut-off (MWCO) of 14 kDa against deionized (DI) water to remove the excess acid until the pH value was 6.

Characterization of Cdots: AFM images were taken by an AFM MultiMode V (Veeco). TEM images were taken on a FEI transmission electron microscope. The zeta potential measurement of Cdots solutions was carried out on a Zetasizer Nano-ZS (Malvern Instruments, UK). Elemental analysis was obtained by using an EA1110CHNO-S (Carlo-Erba) analyzer. The FTIR spectra were obtained by a ProStar LC240 spectrometer. Fluorescence spectra were recorded on a fluoromax-4 spectrofluorometer (HORIBA JOBIN.YVON). UV–vis characterization was conducted on a Lambda 750 UV/Vis/NIR spectrometer (Perkin Elmer. Incs). The photostability of Cdots was tested with a XD300 High Brightness Cold Light (Nanjing Ya Nan Special lighting equipment Manufactory).

Cytotoxicity: The 293T cell line was obtained from the Cell Bank of Chinese Academy of Science and cultured in the standard medium at 37 °C in 5% CO_2. Cells were seeded in a 96-well plate for 24 h before Cdots treatment. Serial dilutions of Cdots with known concentrations were added into cells. After 24 h incubation, the relative viabilities of cell samples were determined by a CellTiter96 kit (Promega) following vendor's protocols. The percentages of viable cells relative to the untreated control were plotted against Cdots concentrations.

In Vivo fluorescence imaging: Female athymic nude mice with the age of 4 to 8 weeks were purchased from Suzhou Industrial

Park Animal Technology Co., Ltd. and were housed in the standard facility. A nude mouse was subcutaneously injected with Cdots-M (2 mg/mL, 20 μL) at three different places on its back after being anesthetized by intraperitoneal injection of 1% pentobarbital. The mouse was imaged by a Maestro in vivo optical imaging system (Cambridge Research & instrumentation, Inc). Varied excitation light wavelengths were applied during imaging. The band-pass widths of the excitation filters are in the range of 20–30 nm.

^{125}I Labeling of Cdots: $Na^{125}I$ was obtained from Chengdu uclear isotope Qualcomm Inc. Cdots-M was labeled by ^{125}I using a standard chloramine T oxidation method.[33,35] A mixture of 500 μL of Cdots-M (2 mg/mL), 600 μCi $Na^{125}I$ and 100 μL 4 mg/mL chloramine-T (Sigma-Aldrich) was reacted in a pH 7.5 phosphate buffer (0.02 M) for 30 min at room temperature. Excess ^{125}I was completely removed by centrifugal filtration through Amicon filters (MWCO = 10 kDa) and washed with water 4–6 times until no detachable gamma activity in the filtrate solution. A radiolabeling yield of 40–50% was achieved. ^{125}I-Cdots-M was injected into mice in the 0.9% NaCl saline solution.

Radiolabeling Stability Test: Approximately 5 μL of ^{125}I-Cdots-M (0.5 mg/mL) was mixed with mouse plasma at 37 °C in a water bath. After different periods of incubation, free iodine was removed by centrifuge filtration through Amicon centrifugal filters (MWCO = 10 kDa) and washed with water for two times. The leftover ^{125}I-Cdots-M after washing was collected for gamma counting to determine the amount of retained ^{125}I on Cdots. Control experiments showed that over 99% of free ^{125}I could be effectively removed by this method.

Blood Circulation and Biodistribution of ^{125}I-Labeled Cdots: Healthy female Balb/c mice were purchased from Suzhou Industrial Park Animal Technology Co., Ltd. All animal experiments were conducted under protocols approved by the Soochow University Laboratory Animal Center. Blood circulation was measured by drawing ~10 μL blood from the tails of Balb/c mice post injection of ^{125}I-Cdots-M. The radioactivity of ^{125}I-Cdots-M in the blood was determined by using a gamma counter (Science and Technology Institute of China in Jia Branch Innovation Co., Ltd.). A series of dilutions of ^{125}I-Cdots-M solutions were measured to obtain a standard calibration curve. For biodistribution measurement, mice injected with ^{125}I-Cdots-M were sacrificed at various time points with major organs collected for gamma counting. All biodistribution data were decay-corrected by the half-life of ^{125}I (60 days). Statistics were based on standard deviations of 5 mice per group. The urine and feces of female Balb/c mice were collected by metabolism cages and measured by the gamma counter after injection of ^{125}I-Cdots-M.

Blood Analysis and Histology Examinations: Twenty-five Healthy female Balb/c mice were injected with 200 μL of 2 mg/mL Cdots-M (a dose of 20 mg/kg) and sacrificed at various time points after injection (1, 7, 20, 40, and 90 days, five mice per time point). Untreated healthy Balb/c mice were used as the control (5 mice per group). An approximately 0.8 mL portion of blood from each mouse was collected for the blood chemistry test and complete blood panel analysis before the mouse was euthanatized. The serum chemistry data and complete blood panel were measured in the Shanghai Research Center for Biomodel Organism. Major organs from those mice were harvested, fixed in 4% neutral buffered formalin, processed routinely into paraffin, sectioned into 8 μm thick slices, stained with hematoxylin and eosin (H&E) and examined by a digital microscope (Leica QWin). Examined tissues include liver, kidneys, spleen, and heart.

Supporting Information

Supporting Information is available from the Wiley Online Library or from the author.

Acknowledgements

This work was partially supported by National Basic Research Program (973 Program) of China (2012CB932600, 2011CB911002), the National Natural Science Foundation of China (51132006, 51002100), and A Project Funded by the Priority Academic Program Development of Jiangsu Higher Education Institutions.

[1] X. Michalet, F. F. Pinaud, L. A. Bentolila, J. M. Tsay, S. Doose, J. J. Li, G. Sundaresan, A. M. Wu, S. S. Gambhir, S. Weiss, *Science* **2005**, *307*, 538–544.
[2] U. Resch-Genger, M. Grabolle, S. Cavaliere-Jaricot, R. Nitschke, T. Nann, *Nat. Meth.* **2008**, *5*, 763–775.
[3] P. V. Kamat, *J. Phys. Chem. C* **2008**, *112*, 18737–18753.
[4] X. Y. Wu, H. J. Liu, J. Q. Liu, K. N. Haley, J. A. Treadway, J. P. Larson, N. F. Ge, F. Peale, M. P. Bruchez, *Nat. Biotechnol.* **2003**, *21*, 452–452.
[5] A. P. Alivisatos, *Science* **1996**, *271*, 933–937.
[6] M. A. Hines, P. Guyot-Sionnest, *J. Phys. Chem.* **1996**, *100*, 468–471.
[7] L.-D. Chen, J. Liu, X.-F. Yu, M. He, X.-F. Pei, Z.-Y. Tang, Q.-Q. Wang, D.-W. Pang, Y. Li, *Biomaterials* **2008**, *29*, 4170–4176.
[8] J. Lovric, S. J. Cho, F. M. Winnik, D. Maysinger, *Chem. Biol.* **2005**, *12*, 1227–1234.
[9] R. Hardman, *Environ. Health Perspect.* **2006**, *114*, 165–172.
[10] P. Lin, J. W. Chen, L. W. Chang, J. P. Wu, L. Redding, H. Chang, T. K. Yeh, C. S. Yang, M. H. Tsai, H. J. Wang, Y. C. Kuo, R. S. H. Yang, *Environ. Sci. Technol.* **2008**, *42*, 6264–6270.
[11] J. Geys, A. Nemmar, E. Verbeken, E. Smolders, M. Ratoi, M. F. Hoylaerts, B. Nemery, P. H. M. Hoet, *Environ. Health Perspect.* **2008**, *116*, 1607–1613.
[12] Y. P. Sun, B. Zhou, Y. Lin, W. Wang, K. A. S. Fernando, P. Pathak, M. J. Meziani, B. A. Harruff, X. Wang, H. F. Wang, P. J. G. Luo, H. Yang, M. E. Kose, B. L. Chen, L. M. Veca, S. Y. Xie, *J. Am. Chem. Soc.* **2006**, *128*, 7756–7757.
[13] L. Cao, X. Wang, M. J. Meziani, F. S. Lu, H. F. Wang, P. J. G. Luo, Y. Lin, B. A. Harruff, L. M. Veca, D. Murray, S. Y. Xie, Y. P. Sun, *J. Am. Chem. Soc.* **2007**, *129*, 11318–11319.
[14] R. L. Liu, D. Q. Wu, S. H. Liu, K. Koynov, W. Knoll, Q. Li, *Angew. Chem. Inter. Ed.* **2009**, *48*, 4598–4601.
[15] D. R. Larson, W. R. Zipfel, R. M. Williams, S. W. Clark, M. P. Bruchez, F. W. Wise, W. W. Webb, *Science* **2003**, *300*, 1434–1436.
[16] H. Peng, J. Travas-Sejdic, *Chem. Mater.* **2009**, *21*, 5563–5565.
[17] H. Zhua, X. Wang, Y. Li, Z. Wang, F. Yang, X. Yang, *Chem. Commun.* **2009**, 5118–5120.
[18] S.-L. Hu, K.-Y. Niu, J. Sun, J. Yang, N.-Q. Zhao, X.-W. Du, *J. Mater. Chem* **2009**, *19*, 484–488.
[19] S. T. Yang, X. Wang, H. F. Wang, F. S. Lu, P. J. G. Luo, L. Cao, M. J. Meziani, J. H. Liu, Y. F. Liu, M. Chen, Y. P. Huang, Y. P. Sun, *J.Phys. Chem. C* **2009**, *113*, 18110–18114.

[20] S. T. Yang, L. Cao, P. G. J. Luo, F. S. Lu, X. Wang, H. F. Wang, M. J. Meziani, Y. F. Liu, G. Qi, Y. P. Sun, *J. Am. Chem. Soc.* **2009**, *131*, 11308–11310.
[21] A. B. Bourlinos, A. Stassinopoulos, D. Anglos, R. Zboril, M. Karakassides, E. P. Giannelis, *Small* **2008**, *4*, 455–458.
[22] A. B. Bourlinos, A. Stassinopoulos, D. Anglos, R. Zboril, V. Georgakilas, E. P. Giannelis, *Chem. Mater.* **2008**, *20*, 4539–4541.
[23] H. P. Liu, T. Ye, C. D. Mao, *Angew. Chem. Inter. Ed.* **2007**, *46*, 6473–6475.
[24] L. Tian, D. Ghosh, W. Chen, S. Pradhan, X. J. Chang, S. W. Chen, *Chem. Mater.* **2009**, *21*, 2803–2809.
[25] Z. H. Kang, H. T. Li, X. D. He, H. Huang, Y. Liu, J. L. Liu, S. Y. Lian, C. H. A. Tsang, X. B. Yang, S. T. Lee, *Angew. Chem. Inter. Ed.* **2010**, *49*, 4430–4434.
[26] K. P. Loh, J. Lu, J. X. Yang, J. Z. Wang, A. L. Lim, S. Wang, *ACS Nano* **2009**, *3*, 2367–2375.
[27] Y. P. Sun, X. Wang, F. S. Lu, L. Cao, M. J. Meziani, P. J. G. Luo, L. R. Gu, L. M. Veca, *J. Phys. Chem. C* **2008**, *112*, 18295–18298.
[28] J. Chen, M. A. Hamon, H. Hu, Y. Chen, A. M. Rao, P. C. Eklund, R. C. Haddon, *Science* **1998**, *282*, 95–98.
[29] Z. Y. Chen, K. Kobashi, U. Rauwald, R. Booker, H. Fan, W. F. Hwang, J. M. Tour, *J. Am. Chem. Soc.* **2006**, *128*, 10568–10571.
[30] Y. P. Sun, J. E. Riggs, Z. X. Guo, D. L. Carroll, *J. Am. Chem. Soc.* **2000**, *122*, 5879–5880.
[31] J. M. Berlin, A. D. Leonard, T. T. Pham, D. Sano, D. C. Marcano, S. Y. Yan, S. Fiorentino, Z. L. Milas, D. V. Kosynkin, B. K. Price, R. M. Lucente-Schultz, X. X. Wen, M. G. Raso, S. L. Craig, H. T. Tran, J. N. Myers, J. M. Tour, *ACS Nano* **2010**, *4*, 4621–4636.
[32] J. M. Berlin, T. T. Pham, D. Sano, K. A. Mohamedali, D. C. Marcano, J. N. Myers, J. M. Tour, *ACS Nano* **2011**, *5*, 6643–6650.
[33] H. F. Wang, J. Wang, X. Y. Deng, H. F. Sun, Z. J. Shi, Z. N. Gu, Y. F. Liu, Y. L. Zhao, *J. Nanosci. Nanotechnol.* **2004**, *4*, 1019–1024.
[34] K. Yang, J. M. Wan, S. A. Zhang, Y. J. Zhang, S. T. Lee, Z. A. Liu, *Acs Nano* **2011**, *5*, 516–522.
[35] S. Zhang, K. Yang, L. Feng, Z. Liu, *Carbon* **2011**, *49*, 4040–4049.
[36] Z. Liu, W. Cai, L. He, N. Nakayama, K. Chen, X. Sun, X. Chen, H. Dai, *Nat. Nanotechnol.* **2007**, *2*, 47–52.
[37] X. Liu, H. Tao, K. Yang, S. Zhang, S.-T. Lee, Z. Liu, *Biomaterials* **2011**, 144–151.
[38] H. S. Choi, W. Liu, P. Misra, E. Tanaka, J. P. Zimmer, B. I. Ipe, M. G. Bawendi, J. V. Frangioni, *Nat. Biotechnol.* **2007**, *25*, 1165–1170.
[39] Reference ranges of hematology data of healthy female Balb/c mice were obtained from Charles River Laboratories: http://www.criver.com/EN-US/PRODSERV/BYTYPE/RESMODOVER/RESMOD/Pages/BALBcMouse.aspx (last accessed Nov 2011).

Received: October 8, 2011
Revised: August 21, 2011
Published online: November 18, 2011

